PHYSICAL REVIEW B VOLUME 21, NUMBER 6 15 MARCH 1980

Dynamics of dense laser-induced plasmas

Ellen J. Yoffa
IBM Thomas J. Watson Research Center, Yorktown Heights, New York 10598
(Received 17 August 1979)

Calculations have been made to determine the influence of a dense plasma of hot electrons and holes on the primary channels of energy relaxation and redistribution of photoexcited carriers in Si, particularly collisions between carriers, plasmon emission, impact ionization, phonon emission, and carrier diffusion. At high carrier densities, Auger recombination is sufficiently fast to ensure that the electrons and holes rapidly reach quasiequilibrium with a common quasi-Fermi level at a temperature which is lowered by the partitioning of energy into thermally excited plasmons. The appropriate dielectric function has been calculated. At sufficiently high temperatures and carrier densities, energy can diffuse at a rate that is comparable to (and, in some cases, faster than) the rate at which the energy is transferred to the lattice. The steady-state carrier density and temperature, and consequently the ultimate extent to which the lattice is heated, depend critically on the parameters of the exciting laser.

I. INTRODUCTION

It has recently been argued that simple-melting or strictly thermal models for pulsed laser annealing of ion-implanted and amorphous Si cannot provide consistent explanations for a large body of experimental evidence.[1-3] It has been suggested as an alternative possibility that annealing is achieved in the presence of an electron-hole plasma.[1,3] In this paper we shall examine a related topic: the dynamics of a dense laser-induced plasma and, in particular, the influence of high concentrations of hot carriers on the rate at which energy is transferred from the laser to the silicon lattice. Previous calculations[4-8] have been performed which assume that the laser energy is transferred to the lattice in the same region in which it is initially absorbed. We shall demonstrate that under certain conditions carrier densities and temperatures are so high that during the laser pulse energy can diffuse from the irradiated volume faster than it heats the lattice. In addition, we shall find that for sufficiently high carrier densities, the phonon emission rate is itself screened. Most theoretical and experimental investigations of energy relaxation on psec to nsec time scales of hot, photoexcited carriers have dealt with carrier densities in Ge (Refs. 9 and 10) and GaAs (Refs. 11–15) which are lower than those at which one would expect the abovementioned effect to occur.

In the following sections, we shall examine the rate at which energy is given to the carriers by the laser, the rates at which carrier collisions redistribute this energy, and the rate at which the energy is transferred to the lattice. In order to compare the relative importance of competing energy-transfer mechanisms, we shall refer our calculations to a typical laser annealing experiment[16] with laser wavelength $\lambda_L = 0.53$ μm, incident power density $P = 10^8$ W/cm^2, and laser pulse duration $\tau_L = 10$ nsec. These parameters correspond to an incident energy density of 1 J/cm^2. Although annealing is often performed in the presence of high implanted donor or acceptor concentrations, we shall assume that any extrinsic carrier densities introduced are small compared with the photoexcited densities.

In Secs. II and III we shall discuss carrier creation and the subsequent thermalization and recombination. The interdependence of the resulting carrier density and energy is examined in Sec. IV. In Sec. V we calculate the effect of a hot, dense plasma on the rate at which energy is transferred to the lattice by phonon emission. In Sec. VI we demonstrate the importance of carrier diffusion in determining the ultimate extent to which the lattice is heated. Finally, in Sec. VII we discuss the implications of our analysis.

II. CARRIER THERMALIZATION

The incident laser energy is absorbed either by electron-hole pair creation or by free-carrier excitation. Initially, with few carriers present, the former process dominates, so that near the silicon surface the photon absorption rate $g = P(1-R)/\delta(\hbar\omega_L)$, where P is the incident laser power per unit area, R is the reflectivity of the sample ($R \approx 0.5$), $\hbar\omega_L$ is the photon energy, and δ is the absorption length ($\delta \sim 10^{-5}$ cm at $\hbar\omega_L = 2.3$ eV). Electron-hole pairs are created via indirect absorption processes involving the emission and absorption of phonons. Because phonon energies are much smaller than the photon energy, the amount of energy transferred to the lattice during absorption is negligible in comparison to the total amount absorbed. The rise in

© 1980 The American Physical Society

carrier density leads, in turn, to increased free carrier absorption. By the same argument as above, we can neglect the energy transferred to the lattice by this process also. The net result is consequently the production of hot electrons and holes which then thermalize with the rest of the carriers and eventually with the lattice. For the example we are considering, $g \sim 10^{31}$ cm^{-3} sec^{-1}, so that carrier densities exceeding 10^{19} cm^{-3} are achieved in times much less than the laser pulse duration. We shall therefore look at carrier thermalization at concentrations greater than 10^{19} cm^{-3}.

Primary channels for energy relaxation of the hot carriers are collisions with the other carriers, plasmon production, and phonon emission. Another important mechanism is electron-hole pair production by impact ionization. (This process is the inverse of Auger recombination, and will be discussed in detail in Sec. III.) Of these processes, all but phonon emission involve primarily the redistribution of the carrier energy among the electrons and holes with negligible amounts of energy transferred to the lattice.

For an electron having an energy E above the conduction-band minimum, the rate of energy loss due to collisions with the N_e other electrons is given by[17]

$$\left(\frac{\partial E}{\partial t}\right)_{e\text{-}e} = -\frac{4\pi N_e e^4 cf}{\epsilon_0^2(2m_e^* E)^{1/2}}, \tag{1}$$

where e and m_e^* are the electron charge and effective mass, and ϵ_0 is the bulk dielectric constant. The energy lost by the hot electron is then shared by all of the carriers. We shall demonstrate in Sec. V that at very high carrier densities, the detailed dependence of ϵ on wave vector $\vec{q}$ and frequency ω becomes important, modifying the simple form of Eq. (1). For the purposes of comparing the relaxation rates, however, simple expressions containing ϵ_0 are adequate. c is a factor between 1 and 2 which accounts for the influence of spin and exchange on a scattering event.[17] f is of order 1, and depends on the distribution of electrons with which the hot electron interacts. Clearly, the importance of the particular distribution diminishes as the energy of the hot electron increases.[17] An expression similar to Eq. (1) applies to electron-hole collisions. As we shall find in Sec. VII, N_e for our example is $\sim 10^{20}$ cm^{-3}, so that with $E \approx 1$ eV, $\epsilon = 11.8$, and $m_e^* = 0.33m$, $(\partial E/\partial t)_{e\text{-}e}$ for our example is roughly -10^{14} eV/sec.

Energy relaxation by plasmon emission is possible when E is greater than $\hbar\omega_p$, where $\hbar\omega_p$ is the plasmon energy,

$$\hbar\omega_p = \hbar\left(\frac{4\pi N_e e^2}{\epsilon_0 m_r^*}\right)^{1/2}, \tag{2}$$

with $m_r^* = 0.15m$ the reduced electron-hole effective mass.[18] The corresponding rate per carrier is[19,20]

$$\left(\frac{\partial E}{\partial t}\right)_{e\text{-}p} = -\frac{(\hbar\omega_p)^2}{a_0(2m_e^* E)^{1/2}} \ln\left(\frac{E}{\hbar\omega_p}\right)^{1/2}, \tag{3}$$

where a_0 is the Bohr radius. Using the values from above for the parameters, $(\partial E/\partial t)_{e\text{-}p}$ is approximately -10^{13} eV/sec. Plasmons can subsequently decay via single-particle excitation (or, if $\hbar\omega_p$ is greater than the energy gap, E_G, by electron-hole pair creation).

For the high carrier densities present ($N > 10^{19}$ cm^{-3}), the plasmon energy $\hbar\omega_p$ is much greater than phonon energies $\hbar\omega$. Consequently, plasmon-phonon coupling is weak and phonon production by the plasmons is negligible. Since no energy is transferred to the lattice by the creation of plasmons and their decay, the energy lost by the hot electron remains in the carrier system. Near the start of the laser pulse, the plasma frequency passes through resonance with the phonons, but the rise in N is so fast that the amount of energy transferred to the phonons in this time is a negligible fraction of the total pulse energy. (With $g \sim 10^{31}$ cm^{-3} sec^{-1}, $\hbar\omega_p$ is resonant with phonon energies for $\sim 10^{-14}$ sec, so that the energy transferred during that time is $\lesssim 5 \times 10^{17}$ eV/cm^3.)

In addition, the carriers may relax by emitting phonons. Again we emphasize that in this process, as opposed to those relaxation channels discussed above, the energy of the hot carrier is not merely redistributed among the remaining carriers but is transferred from the plasma to the lattice. Under the same conditions for which we have estimated the other rates, we shall find $(\partial E/\partial t)_{e\text{-}ph} \sim -10^{11}$ eV/sec. This process will be examined in detail in Sec. V.

Comparing the above results, we find that the rates of energy relaxation by both intercarrier collisions and plasmon production dominate energy relaxation by phonon emission. The reason for this result is that $-(\partial E/\partial t)_{e\text{-}e}$ and $-(\partial E/\partial t)_{e\text{-}p}$ increase with N_e, whereas, as we shall see in Sec. V, $-(\partial E/\partial t)_{e\text{-}ph}$ does not. Clearly, for N_e sufficiently large, the former rates will dominate. This criterion is met for $N_e \geq 10^{18}$ cm^{-3}, so will be satisfied at densities attained in our system.

Arguments analogous to those relevant to electron energy loss rates lead to similar conclusions about hot holes. Consequently, we expect that collisions between carriers result in their rapid thermalization. In times of order 10^{-14} sec, the electrons and holes attain thermal distributions characterized by temperatures $T_e = T_h$. Carrier thermalization is achieved without transferring energy to the lattice, so that the carrier temperature is initially much higher than the temperature of the lattice, T_L.

III. CARRIER RECOMBINATION

Because the carriers are thermalized, both electrons and holes can be described by quasi-Fermi levels and a single temperature $T_e = T_h$. In order to determine the relationship between these two levels we must consider recombination. Auger processes, with rates proportional to N^3, will dominate recombination at high carrier densities.[21] Specifically, an electron recombines with a hole; the energy released is taken up by a third carrier. This hot carrier will rapidly thermalize with the rest of the carriers through collisions and plasmon production as discussed in Sec. II. The Auger rate is given by $(\partial N_e/\partial t)_{\text{Auger}} = -C_e N_e^2 N_h - C_h N_h^2 N_e = -(C_e + C_h) N_e^3 = -CN_e^3$. For crystalline Si, $C \approx 4\times 10^{-31}$ cm^6/sec, where C increases only weakly with temperature.[22]

A sufficiently dense plasma will partially screen the Coulomb interaction between carriers, leading to a modified Auger rate[23]

$$\left(\frac{\partial N_e}{\partial t}\right)_{\text{Auger}} = \frac{-CN_e^3}{[1+(\lambda/k_G)^2]^2} = -C'(N_e)N_e^3\,,$$

where λ is the screening wave vector, and $k_G = (2m_e^* E_G)^{1/2}/\hbar$, with E_G the energy gap, is the approximate wave vector of the most likely recombination transition. As we shall see in Sec. IV, the high carrier temperatures lead to nondegeneracy even at high densities, so that $\lambda^2 \sim N_e$, and the recombination time $\tau_{\text{Auger}} = N_e/(\partial N_e/\partial t)_{\text{Auger}}$ approaches a constant for very large N_e. This screening becomes important at $N_e \sim 10^{21}$ cm^{-3}, and as N_e further increases, τ_{Auger} decreases asymptotically to approximately 6×10^{-12} sec. Carrier excitation occurs at the same time by the inverse process, impact ionization, with $(\partial N_e/\partial t)_{\text{ioniz}} = -C'(N_e)N_0^2 N_e$, where N_0 is the equilibrium value of N_e at T_e.

During the laser pulse, the rate of change of electron density in the irradiated volume is therefore

$$\frac{dN_e}{dt} = \left[\left(\frac{\partial N_e}{\partial t}\right)_{\text{gen}} + \left(\frac{\partial N_e}{\partial t}\right)_{\text{diff}}\right] + C'(N_e)N_e(N_0^2 - N_e^2)\,, \tag{4}$$

where $(\partial N_e/\partial t)_{\text{gen}}$ is the electron laser generation rate and $(\partial N_e/\partial t)_{\text{diff}}$ is the rate at which electrons diffuse from this volume. When $N_e = N_h = N_0$, impact ionization balances Auger recombination, so that the electrons and holes are in equilibrium with each other and are described by a common quasi-Fermi level. We want to find the conditions for which departure from this equilibrium is small. N_0 is a function of the carrier energy density, and therefore varies with time as the laser inputs energy, as energy diffuses away, and as phonons are emitted. N_e follows the changes in N_0 provided the net ionization-recombination rate is faster than the remaining terms in Eq. (4). If $N_e \approx N_0$, Eq. (4) becomes

$$\frac{dN_e}{dt} \approx G + 2C'(N_0)N_0^3 - 2C'(N_0)N_0^2 N_e\,, \tag{5}$$

where $G \equiv (\partial N_e/\partial t)_{\text{gen}} + (\partial N_e/\partial t)_{\text{diff}}$. For N_0 sufficiently large, $2C'(N_0){N_0}^3 > G$. Because $(\partial N_e/\partial t)_{\text{gen}} < g$ (due to free carrier absorption) and $(\partial N_e/\partial t)_{\text{diff}} < 0$, $G < g$. Therefore, when $2C'(N_0)N_0^3 > g$, we can certainly ignore the first term in Eq. (5). This condition is satisfied for $N_0 \gtrsim 10^{20}$ cm^{-3}. In this case, $dN_e/dt \approx -2(N_e - N_0)/\tau_{\text{Auger}}$. As a result, if N_0 does not vary appreciably in times of order τ_{Auger}, N_e will be approximately equal to N_0. Since N_0 is determined by the total energy contained in the carriers, $dN_0/dt < g$, and variations in N_0 are sufficiently slow to ensure that departures from quasiequilibrium are small.

Because Auger recombination need involve no energy loss from the carrier system, the exact details of the absorption of the laser light—i.e., the relative amounts of electron-hole pair excitation and free carrier absorption—are unimportant. The carrier density follows N_0 and is therefore completely determined by the total energy E_{tot} of the carriers.

IV. ENERGY EQUIPARTITION

We can now calculate the dependence of the carrier density and temperature on E_{tot}. N_e equals N_0, so that it obeys the usual expression

$$N_e = \int_0^\infty \frac{g_e(E)\,dE}{1+e^{(E-E_F)/kT_e}}\,. \tag{6}$$

At the same time, the single-particle energy of the electrons is

$$E_e = \int_0^\infty \frac{E g_e(E)\,dE}{1+e^{(E-E_F)/kT_e}}\,. \tag{7a}$$

In Eqs. (6) and (7a), $g_e(E)$ is the single-particle density of states and E_F is the Fermi energy. Equations analogous to these apply to the holes. In addition, energy is stored in thermally excited collective oscillations of the carriers:

$$E_{e\text{-}h} = \left(\frac{k_c^3}{6\pi^2}\right)\frac{\hbar\omega_p}{e^{\hbar\omega_p/kT_e} - 1}\,. \tag{7b}$$

$\hbar\omega_p$ is given by Eq. (2). We assume that these plasmons have negligible k dispersion; $k_c^3/6\pi^2$ is the number of allowed modes at $\hbar\omega_p$. The cutoff wave vector,[19,24] k_c, is taken to be approximately the Debye wave vector,

$$k_c \sim \left(\frac{4\pi N e^2}{\epsilon k T_e}\right)^{1/2} .$$

Assuming ellipsoidal constant energy surfaces characterized by effective masses m_e^* and m_h^*, Eqs. (6) and (7a) become

$$N_e = A_e (m_e^* k T_e)^{3/2} F_{1/2}(\eta) , \tag{8}$$

$$E_e = A_e m_e^{*3/2} (k T_e)^{5/2} F_{3/2}(\eta) , \tag{9}$$

where

$$A_e \equiv \frac{M_e}{2\pi^2}\left(\frac{2}{\hbar^2}\right)^{3/2} ,$$

with M_e the number of equivalent conduction-band minima,

$$\eta \equiv \frac{E_F}{kT_e} ,$$

and

$$F_j(\eta) \equiv \int_0^\infty \frac{x^j\,dx}{e^{x-\eta}+1}$$

is the usual Fermi-Dirac integral. The total energy of the carriers is given by $E_{\text{tot}} = N_e E_G + E_e + E_h + E_{e\text{-}h}$. The term $N_e E_G$ represents the energy of excitation across the gap. We have neglected the dependence of E_G on N_e, T_e, and T_L. However, because the carrier temperature T_e is very high, Eqs. (8) and (9) depend only weakly on E_G and the error introduced is not large. In Fig. 1, we have plotted E_{tot} and $N = N_e + N_h$ as functions of carrier temperature kT_e for Si with parameters $M_e = 6$, $M_h = 1$, $m_e^* = 0.33m$, $m_h^* = 0.55m$, and $m_r^* = 0.15m$.[18] As expected, both number and energy are monotonically increasing functions of temperature.

The importance of the plasmons is not readily apparent from Fig. 1. To demonstrate their role more clearly, we look at the dependence of kT_e on $(E_{\text{tot}} - N_e E_G)/N$, the excess energy per carrier. Using Eqs. (7)–(9), we find

$$\frac{E_{\text{tot}} - N_e E_G}{N} = kT_e \left(\frac{F_{3/2}(\eta)}{F_{1/2}(\eta)}\right) + \frac{e^2}{3\pi\hbar\epsilon}(m_r^* k T_e)^{1/2} \times \frac{z^2}{e^z - 1} , \tag{10}$$

where $z \equiv \hbar\omega_p / kT_e$. kT_e is plotted in Fig. 2 as a function of the per carrier excess energy. For small N, $kT_e \to \frac{2}{3}[(E_{\text{tot}} - N_e E_G)/N]$, as expected. The dashed curve was derived by neglecting the plasmon contribution. Note that the temperature falls below this limit when an appreciable amount of energy is contained in the thermally excited plasma oscillations. This occurs when the carrier temperature and plasmon energies are comparable. In Fig. 3, we plot the fraction of the excess energy contained in the plasmons as a function of carrier temperature. At the peak of the curve, roughly ten per cent of the energy is partitioned into the plasmons. This particular value should not be taken too seriously, however, because it depends critically on our estimate of k_c.

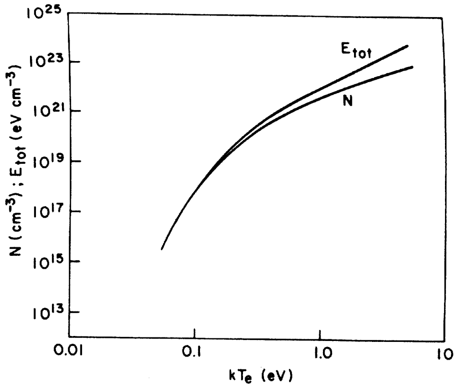

FIG. 1. E_{tot} and N as functions of carrier temperature kT_e calculated for Si with $M_e = 6$, $M_h = 1$, $m_e^* = 0.33m$, $m_h^* = 0.55m$, and $m_r^* = 0.15m$.

For typical doped semiconductors ($N_e \sim 10^{13}$–10^{17}

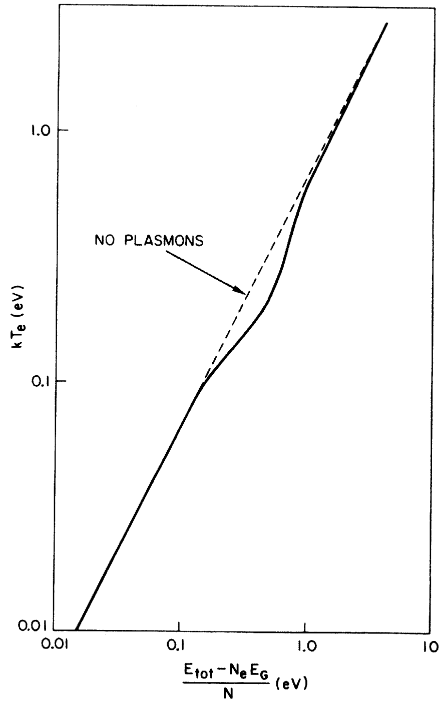

FIG. 2. kT_e as a function of $(E_{\text{tot}} - N_e E_G)/N$. The dashed curve was derived by neglecting the plasmon contribution.

cm^{-3}) at room temperature, $\hbar\omega_p \sim 10^{-4}$–$10^{-2}$ eV $\ll kT$. As a result, many collective modes may be occupied, but their energies are so small they contain a very small fraction of the total energy. For metals, on the other hand, $\hbar\omega_p \sim 10$ eV $\gg kT$. The plasmon energies are very large, but so large that a negligible number of them are thermally excited. It is at just those temperatures ($kT_e \sim 0.1$–1 eV) and densities ($N \sim 10^{19}$–10^{21} cm^{-3}) relevant to our discussion that a significant fraction of the total energy is contained in thermally excited plasma oscillations. The heat capacity of the carrier system is increased as a result of the additional degrees of freedom, into which a significant fraction of the energy is partitioned. In other words, if we try to heat up the carriers by pumping energy into them, their temperature will be lower than in the absence of plasmons, because these modes are absorbing some of the energy.

V. PHONON EMISSION

In this section, we shall first calculate the excitation spectrum for the carrier system and then relate the result to the phonon emission rate. We shall examine this rate in detail, focusing on emission at those $\vec{q}$'s most relevant to silicon, and paying particular attention to the effects of the hot, dense carriers.

We begin by calculating the contribution to the imaginary part of the dielectric function, $\epsilon_2(\vec{q},\omega)$, from electronic transitions within and between conduction-band minima. We do not sum over valence to conduction-band transitions. The ω's at which we ultimately evaluate the dielectric function are far from resonance with interband excitation energies so that these transitions do not contribute significantly to ϵ_2. In the random-phase approximation (RPA),[25]

$$\epsilon_2(\vec{q},\omega) = \frac{4\pi^2 e^2}{\Omega q^2} \sum_{ij} \sum_{\vec{k}\sigma} f^i_{\vec{k}\sigma}(1 - f^j_{\vec{k}+\vec{q},\sigma}) \times \delta(\hbar\omega - [\Delta E(\vec{k},\vec{q})]_{ij}), \qquad (11)$$

where Ω is the volume. The sum $\sum_{ij}$ ranges over all pairs of valleys i and j (including $i=j$) where the transitions are from valley i to valley j. The occupation probability of a state $\vec{k}\sigma$ in the ith valley is $f^i_{\vec{k}\sigma}$ and $[\Delta E(\vec{k},\vec{q})]_{ij}$ is the difference in energy between electronic states $(\vec{k}+\vec{q},\sigma)_j$ and $(\vec{k}\sigma)_i$. In RPA, the electrons have free-electron-like wave functions and polarizabilities, but respond to an effective Coulomb potential which includes screening self-consistently, in contrast to the Hartree-Fock approximation, in which the electrons respond to just the external field.[25]

We approximate each conduction-band minimum by a spherical constant-energy surface having effective mass m_e^*. The wave vector from a particular valley to its jth neighbor is denoted by $\vec{Q}_{oj}$. In this case, we find the following equivalence (see Fig. 4): For any *intervalley* transition $\vec{k} \to \vec{k}+\vec{q}$, there is a corresponding *intravalley* transition $\vec{k} \to \vec{k}+\vec{Q}_j$, where $\vec{Q}_j \equiv \vec{q} - \vec{Q}_{oj}$, such that (a) $f^j_{\vec{k}+\vec{Q}_j} = f^j_{\vec{k}+\vec{q}}$, and (b) $E^j_{\vec{k}+\vec{Q}_j} = E^j_{\vec{k}+\vec{q}}$. Within our approximation for the energy surfaces, the results (a) and (b) follow directly from the definition of $\vec{Q}_j$. [Actually, this equivalence holds exactly in Si for those pairs of *ellipsoidal* valleys aligned on a common (1,0,0) axis.] Equation (11) therefore becomes

$$\epsilon_2(\vec{q},\omega) = \frac{8\pi^2 e^2}{\Omega q^2} \sum_{ij} \sum_{\vec{k}} f_{\vec{k}}(1 - f_{\vec{k}+\vec{Q}_j})\delta[\hbar\omega - (E_{\vec{k}+\vec{Q}_j} - E_{\vec{k}})], \qquad (12)$$

where we have included the intravalley transition by defining $\vec{Q}_{j0,\,\mathrm{intra}} \equiv 0$ so that $\vec{Q}_{j,\,\mathrm{intra}} = \vec{q}$. In Eq. (12), $E_{\vec{k}+\vec{Q}_j} - E_{\vec{k}} = \hbar^2(Q_j^2 + 2kQ_j\cos\Theta)/2m_e^*$, where Θ is the angle between $\vec{k}$ and $\vec{Q}_j$. The important simplification we have made is that we can now include *intervalley* transitions by evaluating the sums within any *one* valley.

The high temperatures ensure that the occupation probabilities are essentially Boltzmann, so that $f_{\vec{k}} \sim e^{-(E_{\vec{k}}-E_F)/kT_e}$ and $f(1-f) \sim f$. Making these substitutions, we obtain

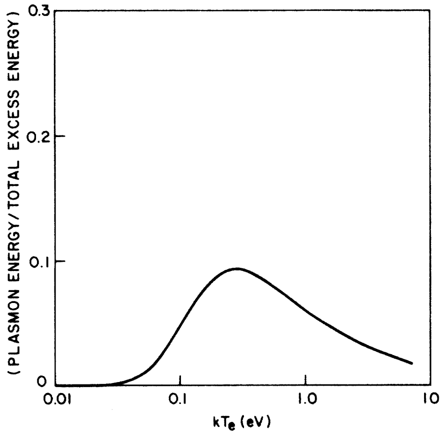

FIG. 3. Fraction of excess carrier energy contained in the plasmons as a function of carrier-temperature kT_e.

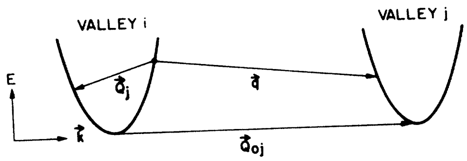

FIG. 4. Schematic of intervalley-intravalley equivalence.

$$\epsilon_2(\vec{q},\omega) = \frac{8\pi^2 e^2}{\Omega q^2} e^{-(E_c - E_F)/kT_e} \sum_{ij} \sum_{\vec{k}} e^{-\hbar^2 k^2/2m_e^* kT_e} \delta\left(\hbar\omega - \frac{\hbar^2}{2m_e^*}(2kQ_j \cos\Theta + Q_j^2)\right), \tag{13}$$

where E_c is the energy of the conduction-band minimum. When we let $\sum_{\vec{k}} \rightarrow (\Omega/8\pi^3)\int d^3k$, sum over i, and integrate over the δ function, Eq. (13) becomes

$$\epsilon_2(\vec{q},\omega) = \frac{M_e e^2}{2q^2} e^{-(E_c - E_F)/kT_e} \sum_j \int_{k_{\min}}^{\infty} \frac{k^2 \exp\left(-\frac{\hbar^2 k^2}{2m_e^* kT_e}\right) dk}{\left|\frac{\hbar^2 k Q_j}{2m_e^*}\right|}, \tag{14}$$

where

$$k_{\min} = \left|\frac{m_e^*}{\hbar^2 Q_j}\left(\hbar\omega - \frac{\hbar^2 q^2}{2m_e^*}\right)\right|.$$

Integrating Eq. (14), we find

$$\epsilon_2(\vec{q},\omega) = \frac{(8\pi)^{1/2}(m_e^* kT_e)^{3/2} M_e}{\hbar^3 q^2} e^{-(E_c - E_F)/kT_e} \sum_j \left(\frac{Z_j e^{-(\hbar\omega - E_{Q_j})^2/4kT_e E_{Q_j}}}{(4\pi k T_e E_{Q_j})^{1/2}}\right), \tag{15}$$

where $E_{Q_j} \equiv \hbar^2 Q_j^2/2m_e^*$, Z_j is the number of valleys separated from valley i by Q_{0j}, and the sum is over normalized Gaussians weighted by Z_j. Finally, using the relation

$$N_e = 2M_e\left(\frac{2\pi m_e^* kT_e}{h^2}\right)^{3/2} e^{-(E_c - E_F)/kT_e},$$

the imaginary part of the dielectric function becomes

$$\epsilon_2(\vec{q},\omega) = \frac{4\pi^2 N_e e^2}{q^2} \sum_j \frac{Z_j e^{-(\hbar\omega - E_{Q_j})^2/4kT_e E_{Q_j}}}{(4\pi k T_e E_{Q_j})^{1/2}}. \tag{16}$$

In Fig. 5, we sketch $\epsilon_2(\vec{q},\omega)$ as a function of $\hbar\omega$ for an arbitrary fixed $\vec{q}$. Note that there are Gaussian peaks centered at $\hbar\omega_j = E_{Q_j}$. These peaks correspond to transitions originating from the densely populated states near the band minima. The widths of the peaks are $(2kT_e E_{Q_j})^{1/2}$. At higher temperatures the peaks are broader because electrons occupy a larger volume in k space, thereby increasing the likelihood of transitions originating from higher in the bands. Of course, the peak heights are complementary to their widths—those resonances that are more spread out are less strong at any given ω.

To put $\epsilon_2(\vec{q},\omega)$ in a more workable form, we approximate the normalized Gaussians by normalized Lorentzians having the same peak locations and widths. Then, using the Kramers-Kronig relations we can obtain $\epsilon_1(\vec{q},\omega)$, the real part of the dielectric function, and, consequently, $\epsilon(\vec{q},\omega) = \epsilon_1(\vec{q},\omega) + i\epsilon_2(\vec{q},\omega)$. This function is

$$\epsilon(\vec{q},\omega) = \epsilon_0(\vec{q},\omega) + \frac{4\pi N_e e^2}{m_e^*} \sum_j Z_j \left(\frac{Q_j}{q}\right)^2 \left(\frac{\omega_j^2 - \omega^2}{(\omega_j^2 - \omega^2)^2 + \omega^2\Gamma_j^2} + \frac{i\Gamma_j \omega}{(\omega_j^2 - \omega^2)^2 + \omega^2\Gamma_j^2}\right), \tag{17}$$

where $\hbar\Gamma_j = (8kT_e E_{Q_j})^{1/2}$. $\epsilon_0(\vec{q},\omega)$ represents the contribution from interband transitions to $\epsilon(\vec{q},\omega)$. As discussed earlier, $\mathrm{Im}\,\epsilon_0(\vec{q},\omega)$ is negligible at those frequencies with which we shall be concerned. Because electron-electron collisions are dominant, collisional broadening widths $\hbar\Gamma_{\mathrm{coll}}$ can be evaluated from Sec. II to be ≈0.05 eV. On the other hand, $\hbar\Gamma_j$ ranges from ≈0.2 eV for intravalley transitions to ≈3 eV for transitions between valleys, so that the collisional widths are very small in comparison and we can ignore them.

Next, we calculate the excitation spectrum

$$\mathrm{Im}\,\frac{1}{\epsilon(\vec{q},\omega)} = \frac{\epsilon_2}{\epsilon_1^2 + \epsilon_2^2}.$$

When we square ϵ_1 and ϵ_2, we find that we can ignore cross terms for differing Q_j, which are negligible (peak times tail) compared to the terms corresponding to the square of one peak. The excitation spectrum is given by

$$\operatorname{Im}\frac{1}{\epsilon(\vec{q},\omega)}=\frac{1}{\epsilon_0}\left[(\hbar\omega_{pe})^2\sum_j Z_j\left(\frac{Q_j}{q}\right)^2\frac{(\hbar\Gamma_j)(\hbar\omega)}{[E_{Q_j}^2-(\hbar\omega)^2]^2+(\hbar\omega)^2(\hbar\Gamma_j)^2}\right]$$
$$\times\left[1+2(\hbar\omega_{pe})^2\sum_j Z_j\left(\frac{Q_j}{q}\right)^2\frac{E_{Q_j}^2-(\hbar\omega)^2}{[E_{Q_j}^2-(\hbar\omega)^2]^2+(\hbar\omega)^2(\hbar\Gamma_j)^2}\right.$$
$$\left.+(\hbar\omega_{pe})^4\sum_j Z_j^2\left(\frac{Q_j}{q}\right)^4\frac{1}{[E_{Q_j}^2-(\hbar\omega)^2]^2+(\hbar\omega)^2(\hbar\Gamma_j)^2}\right]^{-1},\qquad(18)$$

where $\epsilon_0\equiv\epsilon_0(\vec{q},\omega\approx 0)$ and

$$\omega_{pe}\equiv\left(\frac{4\pi N_e e^2}{\epsilon_0 m_e^*}\right)^{1/2}.$$

[ω_{pe} is used for notational convenience and does not correspond to the plasma frequency which is given by Eq. (2).] Earlier, we saw that $\epsilon_2(\vec{q},\omega)$, for fixed $\vec{q}$, was peaked at several values of ω. We now look at Eq. (18) for fixed ω. We find that it is peaked at several q—those q such that $E_{Q_j}\approx\hbar\omega$. (If we had chosen to include hole transitions, the result would simply be the addition here of another peak at $\hbar^2Q_h^2/2m_h^*=\hbar\omega$. However, because all the hole transitions are intravalley, $\vec{Q}_h=\vec{q}$. Since we shall be looking at small $\hbar\omega$, phonon emission by holes therefore occurs primarily at small q. As we shall see, these transitions are well screened even at moderate carrier densities. This will also be the case for intravalley electron transitions, which we can take to be representative of both types of small-q phonon emission.)

In general, each intervalley separation $\vec{Q}_{0j}$ will have a corresponding $\vec{q}$ such that $E_{Q_j}\approx\hbar\omega$. $\operatorname{Im}(1/\epsilon)$ is peaked at these values of $\vec{q}$, which we denote by $\vec{q}_j$. Near these peaks,

$$\operatorname{Im}\frac{1}{\epsilon(\vec{q}_j,\omega)}=\frac{1}{\epsilon_0}\frac{(\hbar\omega_{pe})^2Z_j(Q_j/q_j)^2\hbar\omega(8kT_e\hbar\omega)^{1/2}}{8kT_e(\hbar\omega)^3+(\hbar\omega_{pe})^4Z_j^2(Q_j/q_j)^4}.\qquad(19)$$

The value of $\vec{q}_j$ at each of the peaks corresponds to a particular intervalley transition and, for small ω, $\vec{q}_j\approx\vec{Q}_{0j}$. The widths of these peaks do not vary with q_j, since $\hbar\Gamma_j=(8kT_eE_{Q_j})^{1/2}\approx(8kT_e\hbar\omega)^{1/2}\neq f(q_j)$ for fixed ω.

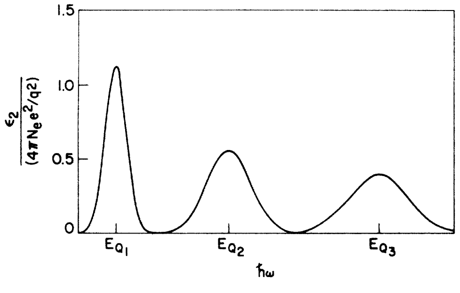

FIG. 5. $\epsilon_2/(4\pi^2N_ee^2/q^2)$ as a function of $\hbar\omega$, for arbitrary fixed $\vec{q}$.

We now relate the excitation spectrum to the phonon emission rate[25]

$$\frac{dN_{\vec{q},\omega}}{dt}=\frac{2\pi}{\hbar}\sum_{ij}\sum_{\vec{k},\sigma}\left|\frac{V_{\vec{k}+\vec{q},\vec{k}}}{\epsilon}\right|^2 f^i_{\vec{k}+\vec{q},\sigma}(1-f^j_{\vec{k}\sigma})\times\delta(\hbar\omega-(E_{\vec{k}+\vec{q}}-E_{\vec{k}})),\qquad(20)$$

where $V_{\vec{k}+\vec{q},\vec{k}}$ is the unscreened matrix element for the transition of an electron from state $\vec{k}+\vec{q}$ to state $\vec{k}$, with the emission of a phonon of wave vector $\vec{q}$. As is usual, we assume V is not a function of the electronic state $\vec{k}$.[26] Evaluating Eq. (20) in the same manner as we did Eq. (12), we find

$$\frac{dN_{\vec{q},\omega}}{dt}=\frac{2\pi}{\hbar}N_e\left|\frac{V}{\epsilon}\right|^2e^{-\hbar\omega/kT_e}\sum_j\frac{Z_je^{-(\hbar\omega-E_{Q_j})^2/4kT_eE_{Q_j}}}{(4\pi kT_eE_{Q_j})^{1/2}}.\qquad(21)$$

Comparing this result with Eq. (16) and using Eq. (17), we see that

$$\frac{dN_{\vec{q},\omega}}{dt}=\frac{m_e^*V^2E_{q_j}}{\pi e^2\hbar^3}\left(\operatorname{Im}\frac{1}{\epsilon(\vec{q}_j,\omega)}\right)e^{-\hbar\omega/kT_e}.\qquad(22)$$

The factor $e^{-\hbar\omega/kT_e}$ appears for phonon emission because carriers must be an energy $\hbar\omega$ higher in the band than required for the absorption transition that contributes to ϵ_2. With the use of Eq. (19), the emission rate can be written as

$$\frac{dN_{\vec{q}_j,\omega}}{dt}=\frac{m_e^*V^2}{\epsilon_0\pi e^2\hbar^3}\times e^{-\hbar\omega/kT_e}\frac{(\hbar\omega_{pe})^2Z_j(\hbar\omega)^2(8kT_e\hbar\omega)^{1/2}}{(\hbar\omega)^38kT_e+(\hbar\omega_{pe})^4Z_j^2(\hbar\omega/E_{q_j})^2}.\qquad(23)$$

Because $\hbar\omega\ll E_{Q_{0j}}$ for intervalley transitions, $\vec{q}_j\approx\vec{Q}_{0j}$. (For transitions within a valley, $\vec{Q}_{0j}=0$, so we treat $\vec{q}_j$ explicitly, with $E_{q_j}\approx\hbar\omega$.) As a result, phonon emission is peaked at those phonons with wave vectors corresponding to the intervalley separations.

$$\frac{dN_{\vec{q}_j,\omega}}{dt}\approx\frac{dN_{Q_{0j},\omega}}{dt}\approx\frac{(\hbar\omega_{pe})^2Z_j(m_e^*V^2/\epsilon_0\pi e^2\hbar^3)e^{-\hbar\omega/kT_e}}{(8kT_e\hbar\omega)^{1/2}[1+(\hbar\omega_{pe})^4Z_j^2/8kT_e\hbar\omega E_{Q_{0j}}^2]}.\qquad(24)$$

In Fig. 6, we sketch $(1/N_e)(dN_{\vec{Q}_{0j},\omega}/dt)$, the rate of phonon emission per electron, as a function of

$(\hbar\omega_{pe})^2$, where we focus on phonons having wave vector $\vec{Q}_{0j}$ and frequency ω. Notice the abrupt change in behavior at

$$(\hbar\omega_{pe})^2 = (\hbar\omega_{pe})^2_{\rm crit} \approx \left(\frac{(\hbar\omega)(E_{Q_{0j}})^2 8kT_e}{Z_j^2} \right)^{1/2} . \tag{25}$$

Since $(\hbar\omega_{pe})^2$ is proportional to N_e, this means that below a critical density of electrons, the per electron emission rate is independent of N_e. In this regime

$$\frac{1}{N_e} \frac{dN_{\vec{q}_j,\omega}}{dt} = \frac{2Z_j V^2 e^{-\hbar\omega/kTe}}{\hbar\epsilon_0[2kT_e(\hbar\omega)]^{1/2}} . \tag{26}$$

However, for sufficiently large N_e, screening by these carriers becomes important and the rate falls rapidly with N_e:

$$\frac{1}{N_e} \frac{dN_{\vec{q}_j,\omega}}{dt} = \frac{m_e^* V^2 E^2_{Q_{0j}} [8kT_e(\hbar\omega)]^{1/2} e^{-\hbar\omega/kT_e}}{\epsilon_0 Z_j \pi e^2 \hbar^3} \left(\frac{1}{(\hbar\omega_{pe})^2} \right) . \tag{27}$$

If $N_e(T_{e1})$ is much less than the critical value given by Eq. (25), then

$$\frac{\left(\frac{1}{N_e} \frac{dN_{\vec{q}_j,\omega}}{dt} \right)_{T_{e2}}}{\left(\frac{1}{N_e} \frac{dN_{\vec{q}_j,\omega}}{dt} \right)_{T_{e1}}} = \frac{\left(\frac{T_{e1}}{T_{e2}} \right)^{1/2} e^{\hbar\omega(1/kT_{e1} - 1/kT_{e2})}}{1 + \frac{[\hbar\omega_{pe}(T_{e2})]^4 Z_j^2}{8kT_{e2}(\hbar\omega)(E_{Q_{0j}})^2}} . \tag{28}$$

We see that for $T_{e2} \gg T_{e1}$, screening by the large number of excited carriers increases the phonon emission time considerably from its unscreened value.

Although the dominant energy loss mechanism is phonon emission by electrons (hole transitions are effectively screened), rapid electron-hole equilibration ensures that both species lose energy at the same per carrier rate,

$$\left(\frac{\partial E}{\partial t} \right)_{e\text{-ph}} = -\frac{\hbar\omega}{N} \sum_j \frac{dN_{\vec{Q}_{0j},\omega}}{dt} \sim -\frac{\hbar\omega}{\tau} . \tag{29}$$

In general, phonon absorption occurs in addition to phonon emission. The net rate of energy relaxation therefore depends on both carrier and lattice temperatures, through terms such as[26] $e^{-\hbar\omega/kT_e} - e^{-\hbar\omega/kT_L}$. In our case, $T_e \gg T_L$, so that there is no explicit dependence on lattice temperature and only phonon emission is important.

We can now evaluate Eq. (25) to find the density at which screening effects become important. Assuming intervalley separations appropriate to crystalline Si,[27-29] there are three classes of transitions for the electrons: (a) Intravalley transitions are represented by $\vec{Q}_0 = 0$ and $Z = 1$. We shall consider phonon emission at $\hbar\omega \approx 0.05$ eV, leading to a corresponding $q = 6.6\times 10^6$ cm^{-1}. (b) All transitions from one valley to another on the same axis can be reduced to one $\vec{Q}_0$, e.g., $\vec{Q}_0 = (2\pi/a)$ (0.4,0,0), where a is the lattice parameter, with $Z = 1$, and $q \approx 4.6\times 10^7$ cm^{-1}. (c) Finally, there are four inequivalent transitions ($Z = 4$) within the first zone from one valley to another on a different axis, e.g., $\vec{Q}_0 = (2\pi/a)$ $(-.2, 1, \pm.2)$ and $(2\pi/a)$ $(-.2, \pm.2, 1)$, so that $q \approx 1.2\times 10^8$ cm^{-1}. For $\epsilon_0(\vec{q},\omega)$ (implicit in ω_{pe}) we use the values calculated by Walter and Cohen.[30] [Although their calculations were performed for $\vec{q}$ along the (1,0,0) direction, and therefore apply strictly only to scattering between valleys on the same axis, we use their results as an estimate of ϵ_0 for off-axis scattering also.]

As a result, Eq. (25) becomes

(a) $(\hbar\omega_{pe})^2_{\rm crit} \approx 0.03(kT_e)^{1/2}$,

(b) $(\hbar\omega_{pe})^2_{\rm crit} \approx 0.85(kT_e)^{1/2}$,

(c) $(\hbar\omega_{pe})^2_{\rm crit} \approx 0.53(kT_e)^{1/2}$,

where the energies are in eV. Using the relationship between N_e and T_e found in Sec. IV, we arrive at the critical densities at which screening begins to become important for (a) intravalley, (b) intervalley, on-axis, (c) intervalley, off-axis scattering, respectively,

(a) $N_{e,\rm crit} \approx 2.5\times 10^{19}$ cm^{-3},

(b) $N_{e,\rm crit} \approx 1.9\times 10^{21}$ cm^{-3},

(c) $N_{e,\rm crit} \approx 1.0\times 10^{21}$ cm^{-3}.

The rates in the strong-screening regime are proportional to $1/N_e^2$, so that, e.g., a factor of 5 increase in N_e reduces the rates by 25. Unscreened energy loss rates are reported to be[28] ~10^{11} eV/sec; from Eq. (24) we see that for $N_e \approx 5\times 10^{21}$ cm^{-3}, the rate may be reduced to ~10^{10} eV/sec. We shall demonstrate in the following section, however, that carrier densities attained

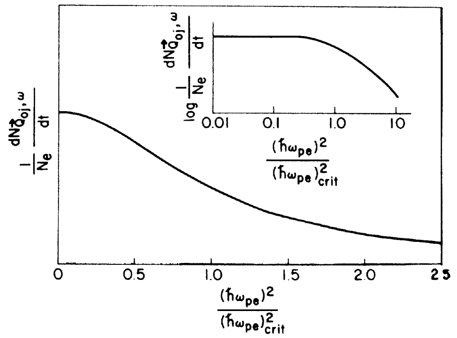

FIG. 6. $(1/N_e)dN_{\vec{Q}_{oj},\omega}/dt$ as a function of $(\hbar\omega_{pe})^2/(\hbar\omega_{pe})^2_{\rm crit}$. The inset shows $\log(1/N_e)(dN_e/dt)$ vs $\log[(\hbar\omega_{pe})^2/(\hbar\omega_{pe})^2_{\rm crit}]$.

are unlikely to exceed the critical densities for screening of intervalley transitions (although screening of intravalley transitions will occur). A reliable estimate of the phonon emission rate depends critically on the electron band structure, which is difficult to determine under extreme conditions of high implantation dosages, amorphization, and rapid atomic rearrangement. Of course, in all of the above calculations we have assumed that the concept of k space is valid and we have evaluated the resulting expressions at those particular values of $\vec{q}$ appropriate to crystalline Si. The strict applicability of this approach depends on the degree of amorphization which itself varies rapidly as a result of the annealing process. As pointed out by Dumke,[31] it may be that transition rates in the noncrystalline state are at least as fast as in the crystal, owing to partial relaxation of selection rules.

VI. CARRIER DIFFUSION

Most of the laser energy is absorbed by the carriers within an absorption depth δ. Eventually, these carriers lose their energy to the lattice; the rise in lattice temperature depends on the distance they have diffused before substantial phonon emission occurs. Now that we know how N_e varies with E_{tot} and the dependence of the phonon emission rate on N_e and T_e, we can examine the manner in which carrier diffusion redistributes the energy. In particular, we shall calculate the effect of diffusion on the rate of phonon emission in a volume near the surface. It is important to emphasize that this is not a simple diffusion process. Although energy is a conserved quantity, the number of carriers is not. When a particular carrier diffuses, it takes its energy with it, thereby reducing the total energy left behind and consequently lowering the carrier temperature. As we have shown in Sec. III, the rapid rate of recombination ensures that N_e is completely determined as a function of time by this temperature. Therefore, N_e decreases not only as a direct result of carrier diffusion but also as an indirect result of the accompanying energy diffusion.

Because of the strong coupling between the electrons and the holes, they must diffuse at the same rate, which is given by

$$\left(\frac{\partial N}{\partial t}\right)_{\text{diff}} \approx D_a \frac{\partial^2 N}{\partial x^2}, \tag{30}$$

where $D_a = 2D_eD_h/(D_e + D_h)$ is the ambipolar diffusion coefficient. We can estimate D_a using the Einstein relation

$$D_a = \left(\frac{kT_e}{e}\right)\left[\frac{2\mu_e\mu_h}{(\mu_e + \mu_h)}\right],$$

where μ_e (μ_h) is the electron (hole) mobility determined by the carrier-phonon scattering time.[32,33] This approximation should yield a reasonable estimate even when carrier-carrier collisions are the dominant interaction, as these collisions do not affect the net plasma momentum. $\mu = e\tau/m^*$, so that $D_a = 2kT_e\tau_e\tau_h/(m_e^*\tau_h + m_h^*\tau_e)$. D_a is therefore ~10^2 cm^2/sec. Because of the exponential dependence of N on T_e, diffusion terms involving $T_e\partial N/\partial x$ are larger than those involving $N\partial T_e/\partial x$ by factors ~$E_G/2kT_e$, so that we are justified in approximating the diffusion by the simple expression Eq. (30).

As a result of carrier diffusion, the carrier energy changes at a rate given by

$$\frac{E_{\text{tot}}}{N}\left(\frac{\partial N}{\partial t}\right)_{\text{diff}} = \frac{E_{\text{tot}}D_a}{N}\frac{\partial^2 N}{\partial x^2}. \tag{31}$$

The equation governing the total carrier energy is then given by

$$\frac{\partial E_{\text{tot}}}{\partial t} = g\hbar\omega_L e^{-x/\delta} + \frac{D_a E_{\text{tot}}}{N}\frac{\partial^2 N_e}{\partial x^2} - \frac{N_e\hbar\omega}{\tau}. \tag{32}$$

The last term represents the rate at which phonons with energy $\hbar\omega$ are emitted. Because $E_{\text{tot}}/N \equiv \langle E_{\text{tot}}\rangle$ and τ are both only weak functions of N_e, the steady-state value of N_e, $N_{e,\text{ss}}$ is

$$N_{e,\text{ss}}(x) \approx \frac{g\hbar\omega_L\tau}{\hbar\omega}\frac{\delta/\alpha}{1-\delta^2/\alpha^2}\left(e^{-x/\alpha} - \frac{\delta}{\alpha}e^{-x/\delta}\right), \tag{33}$$

where $\alpha \equiv (D_\alpha\tau\langle E_{\text{tot}}\rangle/\hbar\omega)^{1/2}$. To obtain this solution, we have used energy conservation via the relation

$$\int_0^\infty g\hbar\omega_L e^{-x/\delta}dx = \int_0^\infty \frac{N_{e,\text{ss}}(x)\hbar\omega}{\tau}dx. \tag{34}$$

At the surface,

$$N_{e,\text{ss}}(x=0) \equiv N_{e,\text{ss}}^0 = \frac{g\hbar\omega_L\tau}{\hbar\omega(\alpha/\delta + 1)},$$

which we can rewrite in the form

$$\frac{N_{e,\text{ss}}^0\hbar\omega}{\tau} = \frac{g\hbar\omega_L}{\alpha/\delta + 1}. \tag{35}$$

Equation (35) directly relates the rate of energy loss by phonon emission to the rate of energy input by the laser. In the absence of diffusion ($\alpha = 0$), the two rates are equal. However, we shall find for our example that α and δ are comparable, so that diffusion reduces the rate of energy transfer to the lattice in the region near the surface.[34]

VII. DISCUSSION

We have evaluated $(\partial E/\partial t)_{e\text{-ph}}$ numerically by using Eq. (28) along with a moderate-density phonon scattering time $\tau \sim 10^{-13}$ sec which is consistent with luminescence data for Si analyzed by Folland[28] and with those values inferred from transport measurements.[35] kT_e and E_{tot} were calculated self-consistently at each N_e as discussed in Sec. IV. Screening does not affect the rate of intervalley phonon emission until $N_e \sim 10^{21}$ cm^{-3}, at which point this rate begins to deviate from its linear N_e dependence. Phonon emission for intravalley transitions falls off at smaller values of N_e. Because screening increases the electron-phonon scattering time, it not only decreases the rate of phonon emission but in addition enhances diffusion. Although for the specific example we are discussing $N^0_{e,\mathrm{ss}} < 10^{21}$ cm^{-3} and therefore screening effects do not play a major role in the rate of energy transfer from the carriers to the lattice, at higher excitation rates these effects can be very important. In Fig. 7 we plot $N^0_{e,\mathrm{ss}}$ as a function of $g\hbar\omega_L$ (cf. Eq. (36)) for the example described in Sec. I. In this case, $g\hbar\omega_L = P(1-R)/\delta \approx 3\times 10^{31}$ eV/cm^3 sec, so that $N^0_{\mathrm{ss}} = 2N^0_{e,\mathrm{ss}} \sim 10^{20}$ cm^{-3}, which is the value we have used for numerical estimates throughout this paper. The fact that $N^0_{e,\mathrm{ss}}$ has turned out to be larger than 10^{19} cm^{-3} justifies our original assumption that the carrier densities are so high that collisions between carriers are the dominant interactions, that the plasma frequency is much larger than phonon frequencies, and that Auger recombination is most important. The dashed line in the figure indicates values of $N^0_{e,\mathrm{ss}}$ obtained by neglecting carrier diffusion ($\alpha = 0$). By comparing the two curves, we see that at a given laser power, diffusion decreases the carrier density near the surface. The rate of energy transfer to the lattice in that region is consequently reduced. Excited carriers may therefore diffuse an appreciable distance from the surface before they give their energy to the lattice, thereby increasing the volume of the region in which this energy transfer occurs.

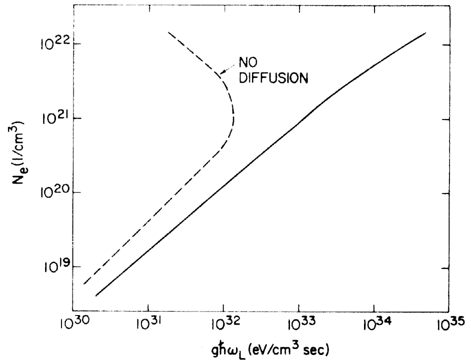

FIG. 7. $N^0_{e,\mathrm{ss}}$ as a function of $g\hbar\omega_L$. The dashed curve was derived by neglecting carrier diffusion.

At high excitation rates, the laser energy is given to the lattice within a characteristic depth determined primarily by carrier diffusion. Owing to the extreme nonlinearity of the hot-carrier effects, the uncertainty in the parameters chosen for our example along with the simplifying assumptions made in our calculations prevents us from making an accurate estimate of the precise temperature to which the lattice is heated or from determining the laser power threshold above which melting will occur. However, because the ultimate temperature rise depends so strongly on the extent of the region in which the energy transfer takes place, carrier diffusion plays a significant role in determining this final temperature.

In summary, we have found that for a photon absorption rate $g \sim 10^{31}$ cm^{-3} sec^{-1} at laser wavelength $\lambda_L = 0.53$ μm and pulse length $\tau_L \sim 10$ nsec, plasmon emission by very hot carriers dominates phonon emission, and collisions between these carriers are so rapid that electrons and holes thermalize in times $\sim 10^{-14}$ sec. Auger recombination, in which the energy remains in the carrier system, is the dominant recombination mechanism at these densities. In times $\sim 10^{-12}$ sec, the electrons and holes recombine, reaching a concentration which then follows changes in the plasma energy. A fraction of the carrier energy is partitioned into thermally excited plasmons, thereby raising the heat capacity of the plasma and decreasing its temperature. By equating the rate at which the energy is given to the plasma to the rate at which energy leaves the carriers via diffusion and phonon emission, we can find the steady-state electron density. For our example, $N^0_{e,\mathrm{ss}} \sim 10^{20}$ cm^{-3}. At this density, only intravalley transitions are effectively screened. Carrier diffusion plays an important role in determining the ultimate extent to which the lattice is heated.

ACKNOWLEDGMENTS

This work was supported in part by the Air Force Office of Scientific Research under Contract No. F49620-77-C-0005. The author is especially indebted to J. A. Van Vechten for suggesting this problem as well as for many stimulating discussions and continual encouragement. She wishes to thank R. C. Frye, W. P. Dumke, P. J. Price, and F. Stern for important suggestions at numerous stages of this work. In addition, the author is grateful to R. Tsu, R. T. Hodgson, R. A. Ghez, A. A. Lucas, and M. H. Brodsky for providing helpful information in their respective areas of expertise.

[1] I. B. Khaibullin, E. I. Shtyrkov, M. M. Zaripov, R. M. Bayazitov, and M. F. Galjautdinov, Radiat. Eff. 36, 225 (1978).

[2] S. I. Romanov, G. A. Kachurin, L. S. Smirov, I. B. Khaibullin, E. I. Shtyrkov, and R. M. Bayazitov, International Conference on Ion Beam Modification of Materials, Paper C12, Budapest, 1978 (unpublished).

[3] J. A. Van Vechten, R. Tsu, F. W. Saris, and D. Hoonhout, Phys. Lett. 74A, 417 (1979); J. A. Van Vechten, R. Tsu, and F. W. Saris, Phys. Lett. 74A, 422 (1979).

[4] R. A. Ghez and R. A. Laff, J. Appl. Phys. 46, 2103 (1975).

[5] J. C. Wang, R. F. Wood, and P. P. Pronko, Appl. Phys. Lett. 33, 455 (1978).

[6] M. Lax, Appl. Phys. Lett. 33, 786 (1978).

[7] J. C. Schultz and R. J. Collins, Appl. Phys. Lett. 34, 84 (1979).

[8] A. Lietoila and J. F. Gibbons, Appl. Phys. Lett. 34, 335 (1979).

[9] A. Elci, M. O. Scully, A. L. Smirl, and J. C. Matter, Phys. Rev. B 16, 191 (1977).

[10] A. Elci, A. L. Smirl, C. Y. Leung, and M. O. Scully, Solid-State Electron. 21, 151 (1978).

[11] J. Shah and R. C. C. Leite, Phys. Rev. Lett. 22, 1304 (1969); J. Shah, Phys. Rev. B 10, 3697 (1974); J. Shah, Solid-State Electron. 21, 43 (1978).

[12] R. Ulbrich, Phys. Rev. B 8, 5719 (1973); R. G. Ulbrich, Solid-State Electron. 21, 51 (1978).

[13] D. H. Auston, S. McAfee, C. V. Shank, E. P. Ippen, and O. Teschke, Solid-State Electron. 21, 147 (1978).

[14] C. V. Shank, R. L. Fork, R. F. Leheny, and J. Shah, Phys. Rev. Lett. 42, 112 (1979).

[15] D. von der Linde and R. Lambrich, Phys. Rev. Lett. 42, 1090 (1979).

[16] R. Tsu, J. E. Baglin, T. Y. Tan, M. Y. Tsai, K. C. Park, and R. Hodgson, *Laser-Solid Interactions and Laser Processing—1978,* Materials Research Society, Boston, AIP Conference Proceedings No. 50, edited by S. D. Ferris, H. J. Leamy, and I. M. Poate (AIP, New York, 1979), p. 344.

[17] C. J. Hearn, Proc. Phys. Soc. 86, 881 (1965).

[18] J. E. Kardontchik and E. Cohen, Phys. Rev. Lett. 42, 669 (1979).

[19] D. Pines and D. Bohm, Phys. Rev. 85, 338 (1952).

[20] J. J. Quinn, Phys. Rev. 126, 1453 (1962).

[21] A. R. Beattie and P. T. Landsberg, Proc. R. Soc. London, Ser. A 249, 16 (1959).

[22] J. Dziewior and W. Schmid, Appl. Phys. Lett. 31, 346 (1977).

[23] A. Haug, Solid-State Electron. 21, 1281 (1978).

[24] D. Bohm and D. Pines, Phys. Rev. 82, 625 (1951).

[25] D. Pines, *Elementary Excitations in Solids* (Benjamin, New York, 1964).

[26] E. M. Conwell, Solid State Phys., Suppl. 9 (1967).

[27] W. P. Dumke, Phys. Rev. 118, 938 (1960).

[28] N. O. Folland, Phys. Rev. B 1, 1648 (1970).

[29] M. H. Jorgenson, Phys. Rev. B 18, 5657 (1978).

[30] J. P. Walter and M. L. Cohen, Phys. Rev. B 5, 3101 (1972).

[31] W. P. Dumke (unpublished).

[32] P. J. Price, Philos. Mag. 46, 1252 (1955).

[33] H. R. Shanks, P. D. Maycock, P. H. Sidles, and G. C. Danielson, Phys. Rev. 130, 1743 (1963).

[34] E. J. Yoffa, Appl. Phys. Lett. 36, 37 (1980).

[35] For a review, see C. Jacoboni, C. Canali, G. Ottaviani, and A. Alberigi Quaranta, Solid-State Electron. 20, 77 (1977).